DEUTSCHES ELEKTRONEN – SYNCHROTRON

DESY 92-028
FTUAM-EP-92-02
February 1992

J/ψ-Production Mechanisms and Determination of the Gluon Density at HERA

H. Jung

III. Physikalisches Institut, Lehrstuhl B, RWTH Aachen

G. A. Schuler

II. Institut für Theoretische Physik, Universität Hamburg

J. Terron

Deutsches Elektronen-Synchrotron DESY, Hamburg

ISSN 0418-9833

NOTKESTRASSE 85 · D-2000 HAMBURG 52

To be sure that your preprints are promptly included in the HIGH ENERGY PHYSICS INDEX, send them to the following (if possible by air mail):

DESY **Bibliothek** **Notkestraße 85** **W-2000 Hamburg 52** **Germany**	**DESY-IfH** **Bibliothek** **Platanenallee 6** **O-1615 Zeuthen** **Germany**

DESY 92-028
FTUAM-EP-92-02
February 28, 1992

ISSN 0418-9833

J/ψ-production mechanisms and determination of the gluon density at HERA[1]

H. Jung[a2], G. A. Schuler[b 3 4], J. Terron[c5].

[a]*III. Phys. Institut, Lehrstuhl B, RWTH Aachen, FRG*

[b]*II. Institut für Theoretische Physik, Universität Hamburg, FRG*

[c]*DESY, Notkestrasse 85, Hamburg, FRG*

Abstract

We discuss photo- and leptoproduction of J/ψ-mesons at energies ranging from fixed-target experiments up to HERA. Elastic and diffractive production as well as various inelastic processes are studied. We investigate the range in which J/ψ-production is described by photon-gluon fusion in the colour-singlet model. We show how inelastic J/ψ production at HERA can be used to extract the gluon density. We estimate an accessible range of $3 \times 10^{-4} < x < 0.1$ and discuss sources of errors in the reconstruction of the gluon density at HERA.

[1]To appear in the Proc. of the workshop on physics at HERA, Hamburg, October 1991, Eds. W. Buchmüller and G. Ingelman.

[2]Supported by Bundesministerium für Forschung und Technologie, 011 5AC 49P, Bonn, FRG.

[3]Supported by Bundesministerium für Forschung und Technologie, 05 4HH 92P/3, Bonn, FRG.

[4]Address after 1.1.92: Theory Division, CERN, CH-1211 Geneva 23, Switzerland.

[5]Partially supported by the exchange programme CICYT-Kfz., Karlsruhe.

1 Introduction

The investigation of J/ψ production is a rich source of information about the dynamics of particle interactions. J/ψ production is well studied in practically all high energy reactions, e^+e^- annihilation, hadronic collisions, deep inelastic scattering and photoproduction experiments. Experiments of the later kinds concentrated on inelastic J/ψ production as a tool to obtain information on the gluon distribution in the proton. Rapidity η and transverse momentum $p_\perp$ distributions were found to be in good agreement [1-4] with photon-gluon fusion into J/ψ plus gluon within the colour singlet (CS) model [5]. The overall normalization, however, is typically off by a factor two to five. Assuming the "K-factor" to be constant in η and $p_\perp$ the gluon distribution of the proton can be extracted from the measured cross section of inelastic J/ψ production. Parametrizing the gluon distribution as $2xG(x) = (1+\eta_g)(1-x)^{\eta_g}$ the NMC collaboration, for example, obtains $\eta_g = 5.1 \pm 0.9$ (stat.) [4].

A rich physics potential can also be explored in elastic and diffractive J/ψ production. These high energy small momentum transfer t processes have different signatures, the J/ψ's being produced in the forward direction with a steep t dependence and isolated in rapidity. Elastic and diffractive processes provide information on the coupling of the photon to the J/ψ meson. Particularly interesting are the prospects to study the nature of the pomeron $\mathbb{P}$ in these reactions.

In this paper we carefully discuss elastic, diffractive as well as inelastic J/ψ production. Extracting the gluon density from inelastic J/ψ production is also one of the goals of HERA. To this end the validity of the CS model has to be investigated in more detail. Two aspects have to be considered: First, the CS model should be extended to include higher order QCD corrections and to account for relativistic effects in the bound state J/ψ meson. Second, alternative production mechanisms have to be investigated.

QCD radiative corrections to the inclusive J/ψ production have not yet been calculated. We shall follow two approaches. In the first case we consider additional production mechanisms besides the CS model and try to identify in which regions of the phase space the individual mechanisms are dominating. When using the CS model we shall take a constant K-factor adjusted to fit the low energy data. A constant K-factor was found to be a reasonable approximation in the case of photo- and hadroproduction of open heavy quarks [7,8] (although being a function of the CM energy). In another approach we give up the CS model completely and try to describe J/ψ production via open charm production. The hadronic final state is transformed into a J/ψ meson if the (sub-) system respecting the J/ψ spin and colour constraints has a mass below the D-meson pair threshold.

A unique feature of HERA is its possibility to measure J/ψ production at widely different energy scales (photon energies). Different production mechanisms have different energy behaviour. From this we expect the discrimination of the various production mechanisms to be possible at HERA.

At the highest photon energy accessible at HERA also processes become significant where $E_{J/\psi} \ll E_\gamma$. Such reactions are described by the scattering of the partonic (quark and gluon) constituents of the photon with those of the proton. We expect these "resolved photon" contributions to J/ψ production to be measurable at HERA for the first time. Their measurements should yield new information on the partonic content of the photon, in particular on its gluon content.

We start by setting up our notation for J/ψ electroproduction:

$$e(l) + p(p) \to e(l') + J/\psi(p_{J/\psi}) + X(p_X) \tag{1}$$

The $ee\gamma$ vertex we describe by the standard DIS variables

$$s = (p+l)^2 \; ; \qquad y = \frac{p\cdot q}{p\cdot l} \; ; \qquad Q^2 = -q^2 \tag{2}$$

where $q = l - l'$ is the four-momentum of the exchanged photon. The $\gamma + p \to J/\psi + X$ subsystem is described by

$$s_{\gamma p} = W^2 = (p+q)^2 \; ; \;\; M^2 = p_X^2 \; ; \;\; z = \frac{p\cdot p_{J/\psi}}{p\cdot q} \; ; \;\; t = (q - p_{J/\psi})^2 \; ; \;\; p_\perp^2 \tag{3}$$

where $p_\perp$ is the J/ψ transverse momentum with respect to the photon axis in the photon-proton CMS.

In this paper we are only interested in cross sections integrated over the azimuthal angle between the lepton and hadron planes. Neglecting the (small) contribution from longitudinally polarized photons, ep cross sections are related to the respective virtual photon proton cross sections via

$$\sigma_{ep}(s) = \frac{\alpha}{2\pi}\int\frac{dy}{y}\int\frac{dQ^2}{Q^2}\left\{\left[1+(1-y)^2\right]\sigma_{\gamma^* p}(W^2,Q^2)\right\} \tag{4}$$

The Q^2 integration limits in (4) are taken exactly as given by the kinematics

$$m_e^2\frac{y^2}{1-y} \le Q^2 \le ys - W_{min}^2 \tag{5}$$

The Q^2 dependence of $\sigma_{\gamma^* p}$ is typically small and we shall neglect it in the following except for cases where a dynamical cut-off restricts the Q^2 range. This happens, for example, in the case where vector meson dominance is used to describe J/ψ production. Here we take:

$$\sigma_{\gamma^* p}(W^2,Q^2) = \left(\frac{m_\rho^2}{m_\rho^2+Q^2}\right)^2\sigma_{\gamma p}(W^2,0) \tag{6}$$

We note that we include the Q^2 dependence of (4) when generating our differential distributions. In particular the p_T distribution of the J/ψ will have a broader tail as compared to the case where the Q^2 dependence is simply omitted. This explains the difference of our p_T distributions with those available in the literature [9], i.e. for J/ψ production in the CS model and J/ψ's coming from b-decays.

The outline of the paper is as follows. First we discuss the dominant J/ψ production mechanisms. We review the CS model and present our models for the additional as well as alternative production mechanisms. Then we compare the models to existing data and present predictions for higher photon energies which are accessible at HERA. Furthermore we discuss additional J/ψ production mechanisms that become visible at the highest photon-proton energies reachable at HERA. We also try to estimate the range in which the CS model can be used to extract the gluon density of the proton. In section 3 we show how to extract the gluon density of the proton at HERA using inelastic J/ψ production. Section 4 contains our summary.

2 J/ψ production mechanisms

At present energies, $\sqrt{s_{\gamma p}} \lesssim 15\,\text{GeV}$, the following four reactions have been observed by photo- and muonproduction experiments [1-4] (Fig. 1):

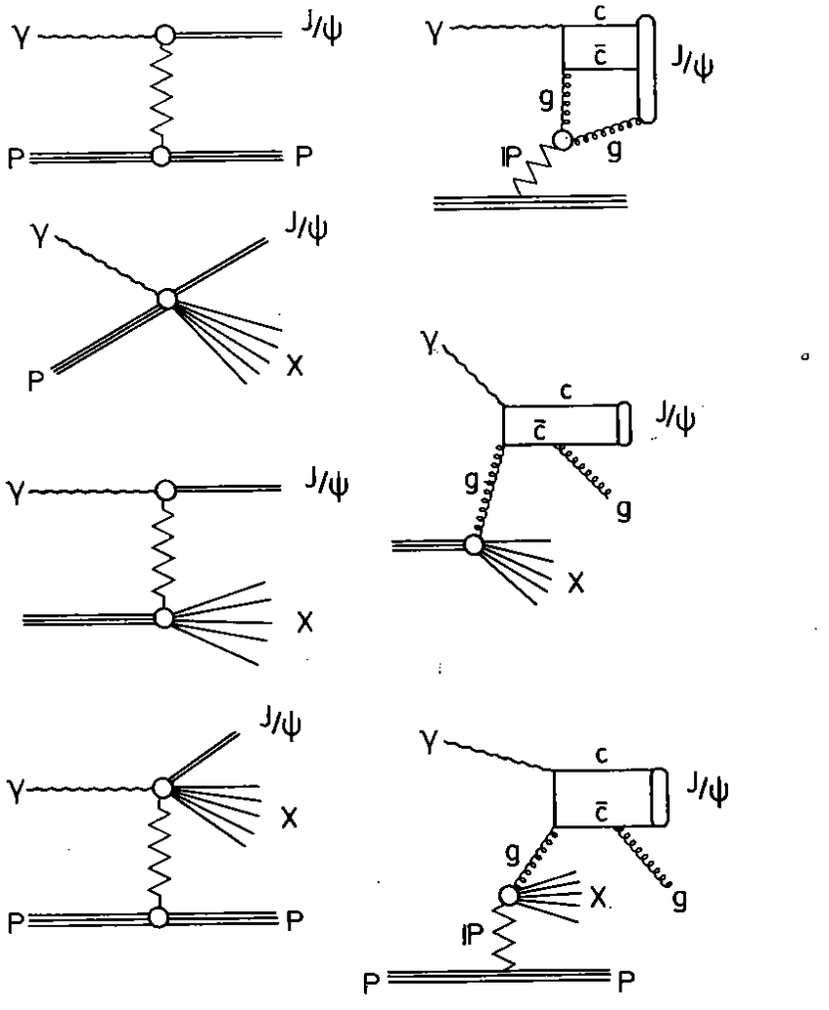

Figure 1: J/ψ photoproduction mechanisms. On the left side the basic processes are sketched and on the right side possible models are shown.

BE + TE: beam elastic and target elastic (elastic)

$$\gamma + p \rightarrow J/\psi + p \qquad (7)$$

BI + TE: beam inelastic and target elastic (diffractive inelastic)

$$\gamma + p \rightarrow J/\psi + X + p|_{diff} \qquad (8)$$

BE + TI: beam elastic and target inelastic (diffractive dissociation DD)

$$\gamma + p \rightarrow J/\psi|_{diff} + X \qquad (9)$$

BI + TI: beam inelastic and target inelastic (direct inelastic)

$$\gamma + p \rightarrow J/\psi + X \qquad (10)$$

Further production mechanisms are expected to become important at higher energies. In particular the so-called resolved photon contributions increase fast with energy. We shall discuss these processes in detail in section 2.6.

The truely inelastic reaction (10), (BI + TI, Fig. 1b) has attracted most interest so far. The process can be calculated perturbatively and is already in leading order sensitive to the gluon distribution of the proton. In the colour-singlet (CS) model [5], (10) is given by the subprocess $\gamma + g \rightarrow J/\psi + g$, c.f. Fig. 1f. This model was found to describe well the differential distributions of inelastic J/ψ-production [1-4]. Both muon- and photoproduction experiments attempted to extract the gluon density from measurements of the differential cross section (10). It is clear that this determination of the gluon density depends crucially on the validity of the underlying perturbative calculation.

In this context one has to discuss the (constant) K-factor that is needed by experiments to achieve agreement with the CS-model. The size of the K-factor is not unusually large ($K \approx 2$–5) when comparing with corresponding ones calculated for e.g. inclusive heavy quark production in hadronic collisions. It is known that these K-factors only weakly depend on the heavy quark rapidity or transverse momentum [7,8]. The case of J/ψ-production is more involved since a bound state system is being produced. The interplay of (relativistic) higher order QCD corrections and the non-relativistic approximation used to describe the bound state is rather difficult and the next-to-leading order calculation is not yet done.

Another observation possibly questioning the CS-model is the excess of events seen at large values of z ($z > 0.9$). Typically a cut on z is made and the CS-model is assumed to be valid and to be the only contributing process below this cut without trying to describe the events at large z. In principle, however, it is possible that the production mechanism responsible for the large z range feeds through towards lower values of z. This would clearly invalidate the ansatz that the lower z region ($z < 0.9$) is given by the CS-model.

In this work we shall report about various approaches that we have started to study the validity of the CS-model and in turn to answer the question whether the gluon density can be extracted from inelastic J/ψ production. These approaches contain models for the additional reactions (7–9) not covered by the CS model as well as a description of J/ψ production based on open charm production.

First there is elastic J/ψ production. Unfortunately the terminology "elastic" is not uniquely used in J/ψ production. The elasticity of the reactions $\gamma + p \rightarrow J/\psi + X$ or

$l + p \rightarrow l + J/\psi + X$ ($l = e, \mu$) is characterized by the dimensionless parameter z (3). Following the FTPS collaboration we define elastic J/ψ production as reaction (7), see Fig. 1a. Correspondingly $z = 1$ apart from tiny mass corrections. In contrast, muon-experiments refer to elastic J/ψ production as events having $z > 0.9$. Note that at high photon energies ν, a small deviation of z from unity provides sufficient energy for the nucleon to break up. Thus elastic J/ψ production à la muon-experiments includes process (9) and possibly also (8). Their parametrization of elastic J/ψ production describes thus a certain combination of (7–9), the precise combination depending on the specific cuts applied in the event selection. For the (true) elastic reaction (7) the total rate is known only from FTPS. We shall describe in section 2.2 models [10,11] that try to predict the t-dependence as well as the energy dependence of (7). The t-dependence as measured by NMC will serve as a check of the models for (7–9).

Besides the elastic process (7) there are the diffractive reactions (8) and (9). In the Regge picture these processes are described by Pomeron $\mathbb{P}$ exchange. In the BI + TE process (8), Fig. 1d, the proton scatters quasi-elastically, i.e. with small momentum transfer and remains intact. The photon is diffractively dissociated in a J/ψ and an additional hadronic system. The relevant subprocess is then $\gamma + \mathbb{P} \rightarrow J/\psi + X$. In a world in which the Pomeron $\mathbb{P}$ is composed out of gluons this reaction can proceed via the $\gamma + g_{\mathbb{P}} \rightarrow J/\psi + g$ subprocess (Fig. 1g) where the gluon stems from the Pomeron. We estimate the BI + TE process in this way in section 2.3 using the CS-model to describe the hard process [10]. Since the beam (i.e. photon) scatters inelastically we expect (8) to contribute to the z distribution similarly as the BI + TI process (10).

For (9) the roles of the photon and the proton are interchanged as compared to (8). The (virtual) photon couples to an off-shell J/ψ-meson which is put on-shell by diffractive scattering off the nucleon which breaks up, Fig. 1c. In section 2.3 we describe a model for (9) based on single-Pomeron exchange and on vector-meson-dominance [11]. Since the photon-J/ψ transition is quasi-elastic we expect the BE + TI process (9) to account for the events at large z. Depending on its absolute rate this process might populate also the low z region conventionally assigned to the CS model.

A completely different approach [10] tries to describe J/ψ-production via open charm production. Early attempts [12] were insufficient because they did not conserve the colour and spin constraints of the J/ψ. For the same reasons also the Drell-Yan type mechanism [13], $q_p + \bar{q}_\gamma \rightarrow g \rightarrow J/\psi$, has to be discarded. Here we propose J/ψ production based on the subset of the $O(\alpha_s^2)$ $\gamma g \rightarrow c\bar{c}g$ matrix elements that give rise to the correct colour and spin state. The $c\bar{c}g$ system is assumed to transform into the J/ψ with unit-probability when its mass is below the threshold of D-meson pair production. Allowing the gluon also to originate from a Pomeron that couples to the proton, in principle all four reactions (7–10) are described in this approach, Fig. 1e–g.

In Tab. 1 we summarize the different production mechanisms together with the models that describe the respective reactions. Regarding the available low energy data, only one experiment (FTPS[1]) has measured separately the four different contributions (TI+BI, TI+BE, TE+BI, TE+BE). In all other cases only combinations have been measured partly because inelasticity was only defined through cuts in z or $p_\perp$.

In the following subsections we shall present models that describe the different reactions quoted above. We start with the totally inelastic contribution, where the CS model and the approach based on open charm production are discussed. Next we consider the elastic and

J/ψ production mechanisms		Model			Data		
		CS	$c\bar{c}(g)$	VMD	FTPS	NA14	NMC
direct inelastic	BI+TI	(11)	(17)		×	×	×
diffractive inelastic	BI+TE	(27)	×		×		
diffractive dissociation DD	BE+TI		(17)	(26)	×	×	×
elastic	BE+TE		(23)	(21)	×		

Table 1: Models for the main contributions to J/ψ photoproduction. The crosses × indicate which model can be used to describe the process and where data are existing. The numbers refer to the equations of the models considered in this article. CS: based on the CS model [5]; $c\bar{c}g$: models based on open charm production [10]; VMD: hadronic like models [11].

diffractive contributions. Then we confront the models with existing measurements. Finally we present the predictions for higher photon energies as they are needed for HERA.

2.1 Inelastic J/ψ production: BI + TI

Inelastic J/ψ-production (10), Fig. 1b, is characterized by a large momentum transfer from the photon to the J/ψ-meson and by a large mass of the remaining hadronic system. Correspondingly the J/ψ-meson is not isolated in rapidity. Due to large scales involved the process can be calculated in the QCD improved parton model. Imposing the colour and spin constraints of the J/ψ-meson on the $c\bar{c}$ system, the hard process in lowest order of the strong coupling constant α_s is (Fig. 1f) $\gamma + g \to c + \bar{c} + g$. Only Feynman diagrams respecting these constraints are to be included. Two approaches exist to transform the open charm state into the bound state J/ψ-meson. In the colour-singlet model the charmed quarks are treated non-relativistically as an s-wave system. The J/ψ wave function at the origin fixes the normalization. In the second approach the charmed quark pair is supposed to transform into a J/ψ if its mass is below the threshold of D-meson pair production. In both approaches inelastic J/ψ-production can be used to determine the target gluon density $G(x)$: it enters the cross section already at the leading order.

2.1.1 Colour-singlet model

In the colour singlet model (CS) [5] photon gluon fusion leads to a colour singlet state in lowest order QCD

$$\gamma(q) + g_1(p_1) \to J/\psi(p_{J/\psi}) + g_2(p_2) \tag{11}$$

where colour is conserved by the emission of gluon g_2. Neglecting the binding energy, the J/ψ can be treated as an S-wave $c\bar{c}$ system. Thus the wave function at the origin $|\psi(0)|^2$ has to be used to predict the absolute normalization. This wavefunction $|\psi(0)|^2$ can be deduced from the measured leptonic decay width of the J/ψ, which in lowest order QCD is given by:

$$\Gamma^0_{l\bar{l}} = 16\pi e_q^2 \alpha_{em}^2 \frac{|\psi(0)|^2}{m^2_{J/\psi}} \tag{12}$$

Including QCD radiative corrections $\Gamma_{l\bar{l}}$ becomes [6]:

$$\Gamma_{l\bar{l}} = \Gamma^0_{l\bar{l}} \left(1 - \frac{16}{3}\frac{\alpha_s}{\pi}\right) \tag{13}$$

The differential cross section for $\gamma p \to J/\psi\, X$ can be written as

$$\frac{d\sigma}{dx\, d\hat{t}} = G(x,\mu^2)\, \frac{d\hat{\sigma}}{d\hat{t}} \tag{14}$$

where $G(x,\mu^2)$ is the gluon distribution function in the proton, μ the mass factorization scale which we shall take as $\mu^2 = \hat{s}$, and $\hat{t} \equiv t$ (3). The differential cross section for the subprocess $\gamma\, g \to J/\psi\, g$ is [5]:

$$\frac{d\hat{\sigma}}{d\hat{t}} = \frac{8\pi\alpha_s^2 \Gamma_{l\bar{l}} m^3_{J/\psi}}{3\alpha_{em}\hat{s}^2} \frac{\hat{s}^2(\hat{s}-m^2_{J/\psi})^2 + \hat{t}^2(\hat{t}-m^2_{J/\psi})^2 + \hat{u}^2(\hat{u}-m^2_{J/\psi})^2}{(\hat{s}-m^2_{J/\psi})^2(\hat{t}-m^2_{J/\psi})^2(\hat{u}-m^2_{J/\psi})^2} \tag{15}$$

where

$$\begin{aligned} \hat{s} &= (q+p_1)^2 = (p_{J/\psi}+p_2)^2 \\ \hat{t} &= (p_{J/\psi}-q)^2 = (p_2-p_1)^2 = t \\ \hat{u} &= (p_{J/\psi}-p_1)^2 = (p_2-q)^2 \end{aligned} \tag{16}$$

Note that the cross section $d\hat{\sigma}/d\hat{t}$ is finite over the whole kinematic range even if $p_2 \to 0$ as a consequence of colour and spin constraints. Throughout this paper we shall use $m_c = 1.5$ GeV, $\mu^2 = \hat{s}$, one-loop expression for $\alpha_s(\mu^2)$ with 4 flavors and Λ given by the structure function and $\Gamma^0_{l\bar{l}}$. Unless otherwise stated we use the parametrization of parton distributions set B1 of [14].

2.1.2 J/ψ-production via open charm production

We now discuss another approach to produce a bound state from a $c\bar{c}$ pair [10]. The matrix element for open charm production [15] $\gamma\, g \to c\bar{c}g$ is used, where we require a colour singlet state for the $c\bar{c}$ pair with the corresponding colour factor. Therefore we include only QED like diagrams, as in the colour singlet model. Through the emission of a final gluon the spin parity of the $c\bar{c}$ pair is fixed. This is in contrast to earlier attempts [12] where the colour and spin constraints were simply ignored. Instead of using the wave function at the origin $|\psi(0)|^2$, the rate of J/ψ production is calculated using the LUND [16] program [6]

$$\begin{aligned} \gamma + g \;\to\; & \underbrace{(c+\bar{c})|_{CS}}_{\to\, J/\psi} + g \end{aligned} \tag{17}$$

Since the matrix element for $\gamma g \to c\bar{c}g$ is not infrared finite, we apply a cut on the $p_\perp$ of the final state gluon ($p_\perp \geq 0.1$ GeV).

[6] In the LUND program a colour singlet system can collaps into a single particle if the invariant mass m of the system is too small to produce two particles (here $m \leq 2m_D$).

2.2 Elastic J/ψ-production

We define elastic J/ψ-production as the reaction (7) in which both the photon ("beam") and the proton ("target") scatter elastically, Fig. 1a. At fixed photon proton CM energy W, the cross section only depends on the momentum transfer t:

$$\frac{d\sigma_{el}(W,t)}{dt} = |f(W,t)|^2 \tag{18}$$

In the simplest ansatz the cross section factorizes

$$|f(W,t)|^2 = |f(W,t=0)|^2 \ e^{Bt} \tag{19}$$

such that B does no longer depend on W. Naively one would expect

$$B = \frac{1}{2}\left(< r^2 >_{J/\psi} + < r^2 >_p\right) \tag{20}$$

Taking the rms radius of the proton to be 0.74 fm and $r_{J/\psi} = r_p/3$ we obtain $B \approx 8$ GeV^{-2}. As we mentioned earlier the only experiment that measured separately the elastic (i.e. BE + TE) process (7) is the FTPS experiment. They quote $\sigma(\gamma p \to J/\psi + p) = 9.8 \pm 1.4(stat.) \pm 1.5(syst.)$ nb. Unfortunately they do not report a value for B.

We describe elastic scattering (7) by single-Pomeron exchange in the Regge picture. The proton-Pomeron-proton ($p-\mathbb{P}-$p) vertex is well studied in proton-proton collisions [17,18,19]. In contrast, the photon-Pomeron-J/ψ vertex is less well known. We discuss two models that have been considered recently to model this vertex. One approach [11] (label VMD in Tab. 1) first links the $\gamma - \mathbb{P} - J/\psi$ vertex to the $J/\psi - \mathbb{P} - J/\psi$ vertex using vector meson dominance ($4\pi\alpha/f^2_{J/\psi} = 1/1570$). Then a Donnachie-Landshoff type Pomeron [17] is being assumed. It is rather an isoscalar $C = +1$ photon which couples to single quarks. The coupling β' of the Pomeron to charm quarks is obtained by comparing the model prediction with the elastic cross section as measured by FTPS. Relating the J/ψ-form factor to the proton form factor by suitably scaling the respective B-parameters the following expression is arrived at

$$\frac{d\sigma_{el}(W^2,t)}{dt} = \frac{4\pi\alpha}{f^2_{J/\psi}} \frac{1}{4\pi} \ (3\beta F_1(t))^2 \ \ (2\beta' F_{J/\psi}(t))^2 (\alpha' W^2)^{2(\epsilon+\alpha' t)} \tag{21}$$

The parameters have the following values:

$$\alpha' = 0.25\,\mathrm{GeV}^{-2} \ , \ \epsilon = 0.085 \ , \ \beta^2 = 4\,\mathrm{GeV}^{-2} \ , \ \beta'^2 = 0.011\,\mathrm{GeV}^{-2}$$

$$F_1(t) = \frac{4m_p^2 - 2.79t}{4m_p^2 - t} \frac{1}{(1 - t/0.71)^2} \ , \ F_{J/\psi}(t) = exp(B_{J/\psi} t) \ , \ B_{J/\psi} = 0.23\,\mathrm{GeV}^{-2} \tag{22}$$

Note that this model not only predicts the energy dependence of the elastic cross section but also an energy dependence for the slope B in (18,19). In section 2.5 we shall show the prediction for the energy dependence of elastic J/ψ production based on this model.

The alternative approach does not rely on VMD but is based on open charm production [10]. Again, the proton scatters elastically through Pomeron exchange. We use the gluonic picture of the Pomeron proposed in [18] and [19] to produce the J/ψ from a hard scattering process. The $\gamma - \mathbb{P} - J/\psi$ vertex is described through the subprocess $\gamma + g_{\mathbb{P}} \to c\bar{c}$ where the

gluon comes from the Pomeron. Elastic J/ψ photoproduction then proceeds via the following mechanism (Fig. 1e)

$$\gamma\,\mathbb{P} \to \gamma\, g_{\mathbb{P}}\, X_{\mathbb{P}} \to c\bar{c}\ X_{\mathbb{P}} \to J/\psi \tag{23}$$

where $X_{\mathbb{P}}$ now stands for the Pomeron remnant, which is a gluon in the simplest case. Since the Pomeron is colour neutral, the $c\bar{c}g$ final state is per definition also colour neutral. In order to produce J/ψ from the final state particles we use again the LUND [16] program.

For the $p - \mathbb{P}$ vertex we use the slightly different parametrization of [20]. It differs from the parametrization of [17] mainly due to a vanishing value for ϵ, c.f. (21) and therefore the cross section stays constant with increasing energy. Defining $r = 1 - x_F^{proton} = M^2/W^2$ we have

$$f_{p\,\mathbb{P}} = \frac{\beta^2_{p\mathbb{P}}(t)}{16\pi} r^{1-2\alpha_{\mathbb{P}}(t)} \tag{24}$$

where

$$\beta_{p\,\mathbb{P}}(t) = \beta_{p\,\mathbb{P}}(0) e^{(-\frac{1}{2}R_N^2 t)} \quad ; \quad \alpha_{\mathbb{P}}(t) = \alpha_{\mathbb{P}}(0) + \alpha'_{\mathbb{P}} t$$

$$R_N^2 = 3.3 GeV^{-2} \ ; \ \beta_{p\,\mathbb{P}}(0) = 10\ \mathrm{GeV}^{-1} \ ; \ \alpha_{\mathbb{P}}(0) = 1 \ ; \ \alpha'_{\mathbb{P}} = 0.3\ \mathrm{GeV}^{-2}. \tag{25}$$

The gluon density in the Pomeron is not well known. Two extreme choices are commonly used: $xG_0(x) = 6\ x\,(1-x)$ when the Pomeron is made from two gluons or $xG_5(x) = 6\,(1-x)^5$ when the gluon is as soft as in the proton. Recent data of UA8 [21] support a gluon density in the Pomeron of the form $xG_0(x)$. Using this gluon density and $m_c = 1.5$ GeV we obtain an elastic cross-section for J/ψ photoproduction at $E_\gamma = 100$GeV of $\sigma = 5$ nb. Note that the K-factor ($K \sim 2$) needed to describe the data is approximately the same as for inelastic J/ψ production. Using $xG_5(x)$ we obtain $\sigma = 0.04$ nb at $E_\gamma = 100$ GeV.

2.3 Diffractive J/ψ-production

Diffractive reactions are the J/ψ production processes BE+TI (9) and BI+TE (8). We compare two approaches to describe the first reaction, BE+TI (Fig. 1c). First we present a model [11] which proceeds via diffractive dissociation of the proton while transforming the photon into a J/ψ meson. Therefore we shall denote the BE+TI process also as DD, i.e. proton diffractive dissociation. Second we show in the next section that the BE+TI process is the high-z part of the inelastic process in the open charm model.

The BI+TE reaction, Fig. 1d, is usually referred to as diffractive production or photon diffractive dissociation. Processes of this kind where the proton remains intact have been studied in the context of jet and open heavy quark production [20]. Here we extend these calculations to the case of diffractive J/ψ production. A model using the gluonic picture of the pomeron supplemented with the CS model is used to describe the BI+TE reaction, c.f. Tab. 1.

We start with the BE+TI process (9), Fig. 1c. The description of elastic $\gamma\,p \to J/\psi\,p$ scattering (BE+TE) in the VMD type model with single Pomeron exchange presented in section 2.2 can be generalized to the BE+TI (= DD) reaction. The main idea is to replace the elastic proton form factor by a suitable integral over the inelastic structure function $\bar{F}_2$. The latter deviates from the standard structure function $F_2(x,Q^2)$ in that the quark distributions functions are not weighted with their charge squares according to the different couplings of the photon and the Pomeron to quarks. We use the $\bar{F}_2(x,Q^2)$ parametrization

of [17]. Then the following formula for the differential DD cross section is arrived at [11]:

$$\frac{d\sigma_{DD}}{dt\,dM^2} = \frac{4\pi\alpha}{f_{J/\psi}^2}\frac{1}{4\pi M^2}(2\beta' F_{J/\psi}(t))^2(\frac{s}{M^2})^{2(\epsilon+\alpha' t)}(1-\frac{M^2}{s})\beta^2\tilde{F}_2(x,|t|) \qquad (26)$$

where $x = |t|/(M^2+|t|-m_p^2)$. Note that the whole set of parameters in (26) is fixed. Thus (26) is a definite prediction for the BE+TI reaction. The FTPS experiment quotes a value $\sigma(\gamma p \to J/\psi|_{diff}+X) = 4.4 \pm 0.9(stat.) \pm 1.1(syst.)$ nb which is to be compared to the model prediction at low energies of $\sigma(\gamma p \to J/\psi|_{diff}+X) = 2.8$ nb.

In the BI + TE process (8), Fig. 1d, we assume the proton to scatter quasi-elastically via Pomeron exchange. Here we take the gluonic picture of the Pomeron $\mathbb{P}$ [19]. We then describe the inelastic $\gamma + \mathbb{P} \to J/\psi + X$ subprocess as a convolution of the gluon density $g_{\mathbb{P}}$ in the Pomeron with the hard partonic process

$$\gamma + g_{\mathbb{P}} \to J/\psi + g_2 \qquad (27)$$

The latter we evaluate in the CS model. Since the relevant subprocess describes inelastic J/ψ production, we call this process also diffractive inelastic J/ψ production in order to distinguish it from the ordinary inelastic process where the gluon comes directly from the proton. One could argue that the diffractive inelastic process constitutes a part of the ordinary inelastic process rather then being an independent new contribution [19]. In any case, we expect the BI+TE reaction to be small. Taking the above model we find at FTPS energies $\sigma(\gamma + p \to J/\psi + p|_{diff}+X) = 0.1$ nb when using $xG_{\mathbb{P}}(x)$. This is consistent with the number quoted by the FTPS experiment [1], $\sigma_{exp} < 0.7$ nb.

2.4 Comparison with Data

In Fig. 2 we compare the z-distribution of the CS model (section 2.1.1) for photoproduction of J/ψ with data from FTPS [1], NA14 [2] at $E_\gamma = 100$ GeV and NMC [4] ($E_\gamma \sim 150$ GeV). The NMC data for $\mu p \to J/\psi X$ are compiled to photoproduction $\gamma p \to J/\psi X$ using the method described in [3], resulting in $\sigma_{\gamma p} = 69.4\ \sigma_{\mu p}$ for the total cross section at a mean photon energy of $E_\gamma = 150$ GeV. From Fig. 2 we see that the shape of the z-distribution of the CS model fits quite well with all experiments in the region below $z \sim 0.9$. We recall that for fixed target experiments z is the scaled J/ψ-energy, $z = E_{J/\psi}/E_\gamma$. Yet, note that different normalization factors K are needed in order to achieve agreement between the CS model and the data at $z < 0.9$: $K[FTPS] = 1.8$, $K[NA14] = 3.7$, $K[NMC] = 4.9$ when using lowest order Γ^0_{ll}, $\alpha_s = 0.3$ and $xG(x) = 3(1-x)^5$. Using the parameters of the CS model as specified in section 2.1.1 we obtain the following K-factors: $K[FTPS] = 2.8$, $K[NA14] = 5.6$, $K[NMC] = 6.8$. Including the radiative corrected Γ_{ll} the respective K factors are reduced by about a factor two. Even though there are large systematic uncertainties in the experimental data points, the discrepancies between photo and muon production experiments presumably arise mostly from differences in the definition of the inelastic domain. The NA14 and FTPS collaborations try to remove diffractively and elastically produced J/ψ's through the requirement of at least one additional track. No such cut is applied in the NMC analysis. Despite of the large K factor one usually concludes from Fig. 2 that inelastic J/ψ production is well described by the colour singlet model in the region $z \leq 0.9$. This statement is supported by the observation of NMC that for $z \leq 0.9$ the distribution in the J/ψ transverse momentum agrees with the data

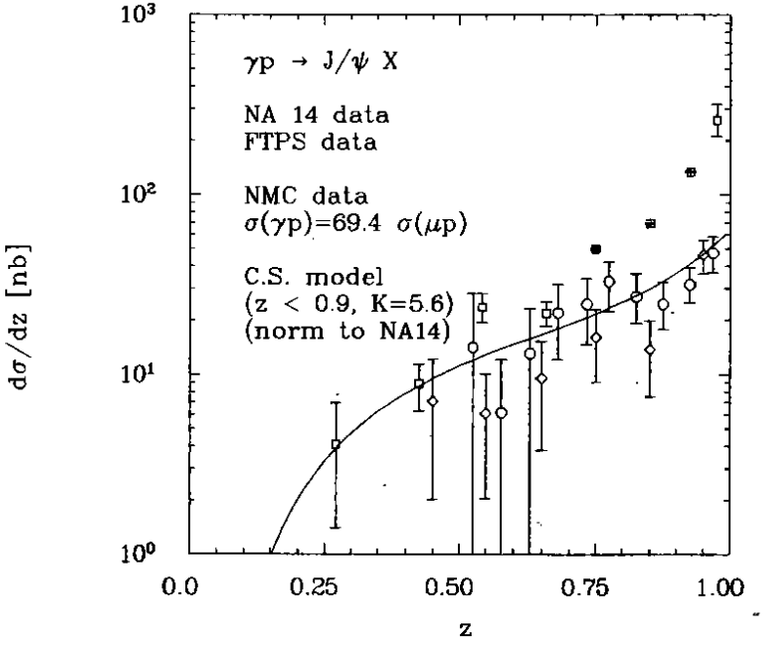

Figure 2: z distribution for J/ψ photoproduction calculated in the CS model (section 2.1.1) compared to data from FTPS($\diamond$), NA14 ($\circ$) at $E_\gamma = 100$ GeV and NMC($\Box$) at $E_\gamma = 150$ GeV The CS- model is multiplied by $K = 5.6$ in order to fit the NA14 data.

down to $p_{\perp J/\psi}^2 \geq 0.1\,\text{GeV}^2$. Here a cut $M^2 > 10\,\text{GeV}^2$ has been applied in order to suppress elastic and diffractive contributions.

As mentioned earlier we are still lacking the complete next-to-leading order calculation of inelastic J/ψ production. In order to investigate the ansatz of J/ψ production via photon gluon fusion we study now inelastic J/ψ production in the open charm approach as introduced in section 2.1.2. In Fig. 3 we compare the alternative J/ψ production via open charm production with data from NMC. For easier reference we also show the result of the CS model. A cut $p_\perp \geq 0.1$ GeV is applied to both models. The open charm approach not only describes the shapes of the distributions quite well but also provides an estimate for the cross section, which is comparable to that obtained from the CS model. It should be noted that the same K factor is applied to both models in Fig. 3.

From Figs. 2 and 3 we find that the discrepancy between the CS model and the muon production data at large z ($z > 0.9$) can not be accounted for by a constant K factor. This indicates the limit of validity of the CS-model. At large z the emitted gluon becomes very soft and the J/ψ scatters more and more elastically. A description of J/ψ production based on the emission of a single gluon as is done in the CS model is no longer appropriate. Effects of multiple soft gluon emission have to be considered. Then many more ways are open to arrange the proper colour and spin state. Therefore the CS model has to fail at large z.

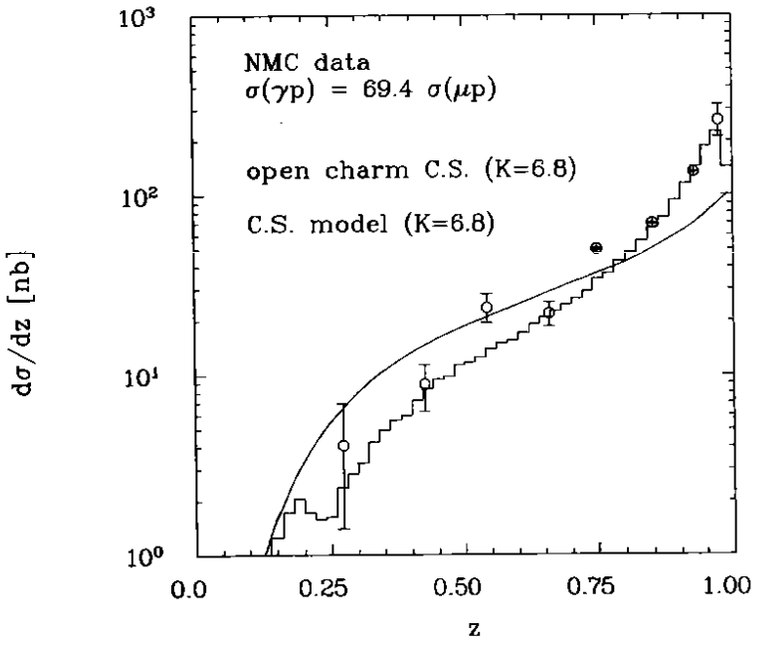

Figure 3: z distribution of J/ψ photoproduction at $E_\gamma = 150\,\text{GeV}$ in the open charm approach (section 2.1.2, histogram) and in the CS model (solid line) together with NMC data. Both models are multiplied by $K = 6.8$.

In contrast, the approach based on the $O(\alpha_s^2)$ open charm matrix elements shows the $\frac{1}{1-z}$ behaviour which is typical for soft gluon bremsstrahlung. For z not too close to unity this behaviour should correctly describe the soft gluon effects. Eventually a summation of the $\frac{1}{1-z}$ terms has to be performed. Here we regularize the apparent singularity at $z = 1$ by the cut $p_\perp > 0.1\,\text{GeV}$ which restricts z to values smaller than unity. From Fig. 3 we find that the open charm approach describes the large z events of NMC remarkably well. There is nearly perfect agreement with the data although no fit has been performed and the same K factor is used as in the CS model. As z approaches unity (from below) the whole $c\bar{c}g$ system collapses into the J/ψ. Thus the open charm model describes actually BE+TI scattering as $z \to 1$.

A somewhat different z distribution for the BE+TI events is predicted by the hadronic like model of section 2.3. In Fig. 4 we show the z distribution of the BE+TI or DD process[7] as obtained from (26) together with the result of the CS model. Here we compare with data from FTPS. The CS model is multiplied by $K = 2.8$ in order to describe the FTPS data. The characteristics of the z distribution (Fig. 4) of the DD process (9) as predicted by (26) are similar to the ones obtained in the open charm approach: The z distribution peaks[8] at large z and is falling fast as z decreases. The main difference is the steeper slope in the hadronic

[7]The elastic process (7) is not shown since it is a delta function like contribution at $z = 1$.

[8]In contrast to the open charm model the cross section remains finite at $z = 1$ in the hadronic model.

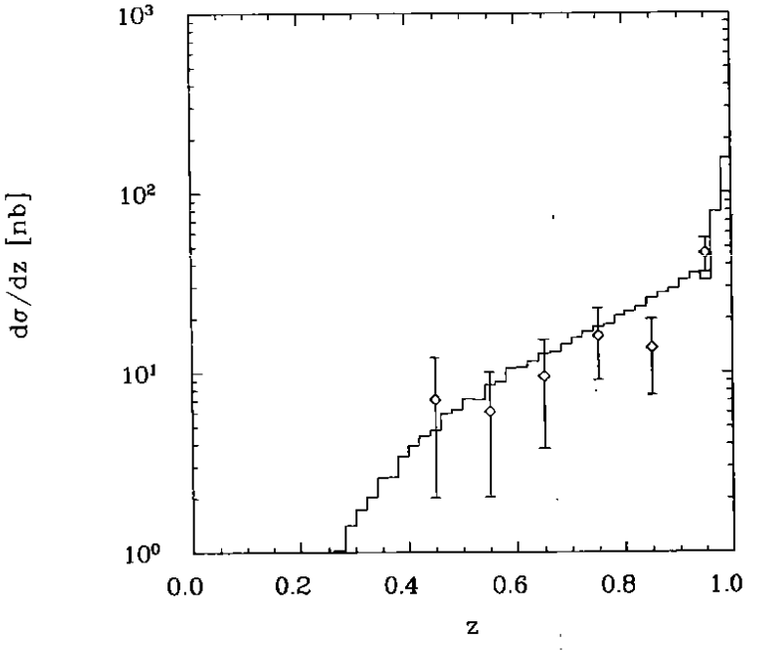

Figure 4: z distribution of inelastic J/ψ photoproduction at $E_\gamma = 100\,\text{GeV}$ in the CS model ($K = 2.8$) and for diffractive J/ψ production through the BE+TI (= DD) mechanism (26). The two models are matched as given by eq.(28). For comparison data points of FTPS are shown.

model. As can be seen in Fig. 4 the DD process (9) as modeled in (26) precisely describes the FTPS data at large z, i.e. the region $0.9 \leq z < 1$ (at $E_\gamma = 100\,\text{GeV}$). Furthermore, the diffractive reaction smoothly matches the inelastic process (10) as given by the CS model.

We conclude that the region $z < 0.8$ - 0.95 defines the domain of inelastic J/ψ production. Within this range inelastic J/ψ production is described by photon gluon fusion and in turn can be used to extract the gluon density. Apart from a constant K factor the CS model describes the inelastic data. All differential distributions agree also with the model based on open charm production. The diffractive reaction (9) is confined to the large z region and has different signatures: steeper distributions both in t and z and the J/ψ isolated in rapidity. The open charm approach predicts a bremsstrahlungs like spectrum in the limit $z \to 1$ as it seems appropriate for the NMC data. The hadronic like model (26) gives a steeper z distribution which seemed preferred by the FTPS data.

In any case, the CS model multiplied by a suitable K-factor plus the diffractive reaction (9) describe completely the existing (low energy) data. The prediction for the transition region between the CS model and the DD process is somewhat model dependent. In the hadronic model the transition happens at $z \simeq 0.95$. At higher energies the transition, i.e. the validity region of the CS model, is predicted to extend towards larger values of z. This

prediction is based on the analysis in [11] where it was found that the boundary between the CS model and the DD reaction is approximately given by

$$M^2 \approx 8 \left(\frac{W^2}{200\,\mathrm{GeV}^2} \right)^{0.7} \mathrm{GeV}^2 \qquad (28)$$

The measurement of the z distribution of J/ψ production at different CM energies would be a very powerful tool to study the underlying dynamics.

So far we have not shown results for the BI+TE process which we model by $\gamma + g_{\mathbb{P}} \rightarrow J/\psi + X$. The reason is that at fixed target energies the BI+TE reaction is very small, less than 3% at FTPS [1]. In our model (section 2.3) the z dependence of this reaction is the same as for the CS model. In addition as mentioned above, the BI+TE process might be considered as part of the inelastic reaction.

2.5 J/ψ production at high energies

At HERA it will be possible to measure γp cross sections over a wide range in the photon energy. Measurements of the energy dependence of J/ψ production will allow to discriminate between different models and to study the reactions (7-10) in detail. The $\sqrt{s_{\gamma p}}$ dependence of the respective γp cross sections is shown in Fig. 5. The inelastic J/ψ production (10) is calculated in the CS model for two different parametrization of the gluon density. A K factor of $K = 2.8$ has been applied. The result for the elastic cross section (7) is shown for model (21) [11] only, since the parametrization of the pomeron $\mathbb{P}$ as used in the other model (23) [10] gives a constant cross section. Also shown are the diffractive reactions, the DD process (26) and the BI+TE reaction (27) as described in section 2.3. We find that the elastic reaction is of similar size as the inelastic production. The estimates of the different approaches differ significantly as $\sqrt{s_{\gamma p}}$ increases. Thus measurements of the energy dependence of (7-10) at HERA will allow to discriminate between the individual descriptions. Besides different energy dependences further differences are expected in the angular distribution of the J/ψ. Useful information about the photon J/ψ coupling as well as about the structure of the Pomeron can thus be obtained from those measurements.

The NMC collaboration fitted the energy and t dependence of J/ψ production at $z > 0.9$. They obtain (c.f. (18,19):

$$|f(W, t=0)|^2 = 1.2\, a\, \exp\left\{ \frac{-b}{\nu - c} \right\} \qquad (29)$$

where $a = 20\,\mathrm{nb}$, $b = 45\,\mathrm{GeV}$, $c = 6\,\mathrm{GeV}$ and $\nu = ys/(2m_p)$. Furthermore they obtain a value of 1.2 for B much smaller than the naive expectation (20) and also smaller than the value $B = 4.3$ obtained in the model of eq.(21). The reason is that their event selection $z > 0.9$ not only includes elastic J/ψ production (7) but also contributions of the diffractive reactions (8) and (9). These processes have smaller values for B: $B[DD] = 1.7$. In fact, the sum of (21) and (26) yields a t dependence closer to the NMC measurement [11], $B[sum] = 2.4$. The energy dependence of the $z > 0.9$ events as fitted by NMC is also shown in Fig. 5.

The BI+TE process has a small cross section at present energies ($\sqrt{s_{\gamma p}} \leq 15$ GeV) and only an upper limit exists from FTPS, c.f. section 2.3. As can be seen from Fig. 5 we predict an observable rate at maximal HERA energies offering the prospects of direct measurements

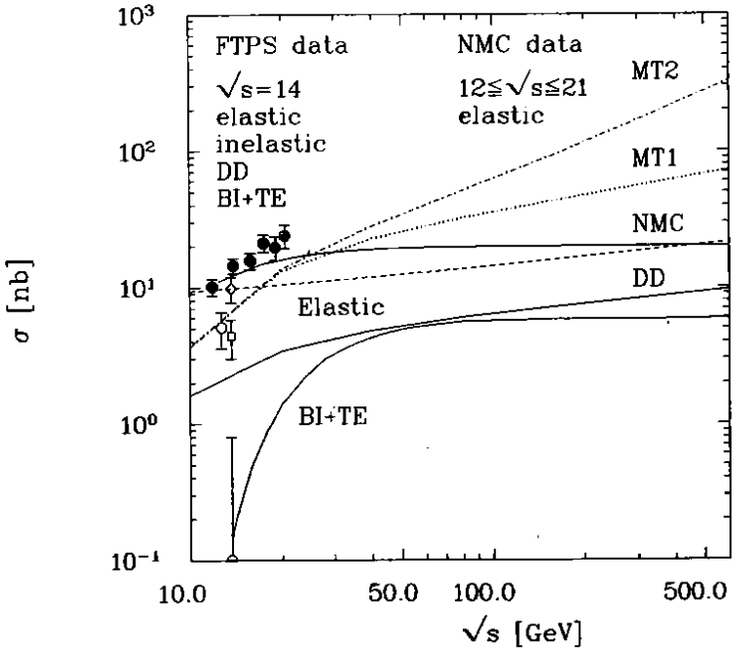

Figure 5: CM energy dependence of the dominant J/ψ photoproduction mechanisms (7–10). Inelastic production (10) in the CS model ($K = 2.8$) for two different gluon density functions of Morfin and Tung: set B1 (dotted), set B2 (dash-dotted). Elastic J/ψ production (7) as predicted by the hadron like model (21) labeled *elastic* in dashes. The solid lines show the results of diffractive J/ψ production: the DD process as predicted by (26) and BI+TE scattering described by (27). Inelastic and DD production are separated according to eq. (28). The curve labeled NMC gives the parametrization of NMC (29). The open data points are: FTPS BE+TE(◇), FTPS BE+TI(□), FTPS BI+TE(◦ upper limit), FTPS BI+TI(◦) and the black points NMC elastic (•).

of the gluon density in the Pomeron. Although the diffractive inelastic process BI+TE is smaller than the direct inelastic process (10) it could be isolated by tagging the scattered proton and /or by measurements of the hadronic energy flow. The rapidity distribution of the hadronic particles at HERA is shown in Fig. 6 for hard diffractive inelastic ($\gamma g_{\mathbb{P}} \rightarrow J/\psi g$) and direct inelastic ($\gamma g_p \rightarrow J/\psi g$) J/ψ production. The diffractive production provides a very clean signature through the rapidity gap between the proton and the hadronic particles coming from the fragmentation of the gluons.

We summarize the cross sections of the various J/ψ production processes in ep collisions at HERA in Tab. 2. These are cross sections without cuts. Note that the cross sections are normalized to low energy data (with the given K factors).

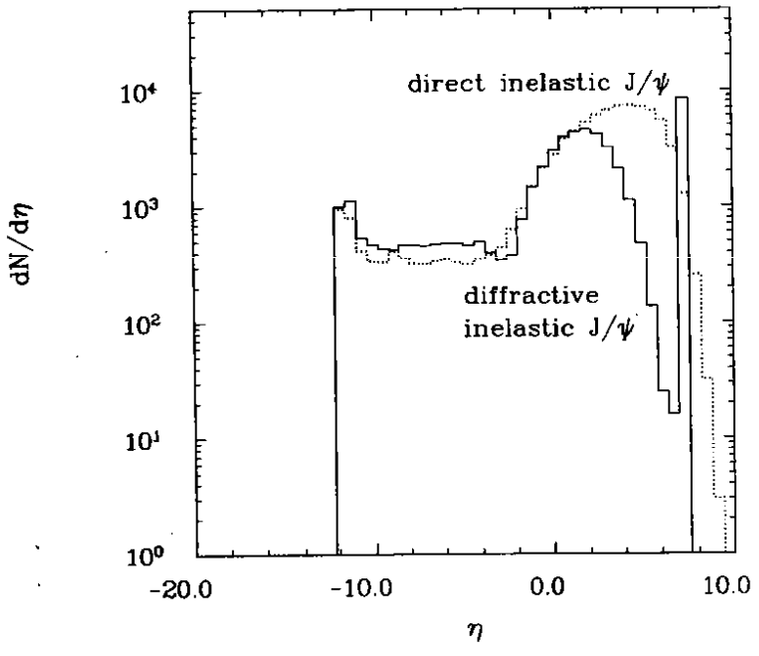

Figure 6: Rapidity distribution of the hadronic system for inelastic J/ψ production at HERA. Dotted line: the direct production BI+TI in the CS model (11); solid line: diffractive inelastic production BI+TE (27).

Process	Elastic		DD	direct inelastic	diffractive inelastic
Equation	(23) ($K=2$)	(21)	(26)	(11) ($K=2.8$)	(27)
σ	2.20 nb	4.49 nb	1.40 nb	8.30 nb	0.35 nb

Table 2: Contributions to the electroproduction of J/ψ at HERA without cuts and normalized to low energy data with the given K factors. Inelastic and DD production are separated according to eq. (28).

2.6 Additional J/ψ production mechanisms

At the rather low energies reachable at fixed target experiments [1-4], J/ψ's can only be produced by elastic and diffractive processes and the direct inelastic process (11). Additional inelastic production mechanisms are expected to become measurable at HERA energies:

resolved photon contributions: direct J/ψ production

$$g + g \;\rightarrow\; J/\psi + g \tag{30}$$

$$g + g \;\rightarrow\; J/\psi + \gamma \tag{31}$$

resolved photon contributions: χ decays

$$\begin{aligned} g + g &\rightarrow \chi_{0,2} \rightarrow J/\psi + \gamma \\ \{gg, q\bar{q}\} &\rightarrow \chi\,(\rightarrow J/\psi + \gamma) + g \\ gq &\rightarrow \chi\,(\rightarrow J/\psi + \gamma) + q \end{aligned} \tag{32}$$

two photon contributions [9].

$$\gamma + \gamma \rightarrow \chi_{0,2}(\rightarrow J/\psi + \gamma) \tag{33}$$

b decays

$$(\gamma, g) + g \rightarrow b\bar{b} \rightarrow J/\psi + X \tag{34}$$

double charm production

$$(\gamma, g) + g \rightarrow J/\psi + c\bar{c} \tag{35}$$

At low virtuality (low Q^2) the photon not only couples directly to the partons within the nucleon. There is a certain probability for the photon to behave like a hadron giving rise to the so-called resolved photon contributions. Hard processes and/or production of heavy objects receive then contributions from parton parton scatterings where one parton stems from the proton and the other from the photon, c.f. (30-32). Throughout this paper we use the parametrization for the photon contents of [22]. In Fig. 7 we compare the energy dependence of inelastic photoproduction of J/ψ mesons through direct photon coupling as described in the CS model and J/ψ production through the resolved photon contributions (30) and (32). The latter are very much suppressed at low energies but increase very rapidly with energy. We expect these contributions to J/ψ production to become measurable at HERA for the first time. The main subprocesses are the gg initiated ones, $gg \rightarrow J/\psi\, g$ and $gg \rightarrow \chi_{1,2}\, g$. These processes could be used to obtain information about the gluon density function in the photon. To this end the process (31) might be very useful. As observed in [23] the $J/\psi + \gamma$ final state is not only very clean. Moreover, the gluon initiated subprocess (31) is the only contributing process in leading order providing in principle a unique handle on $xG_\gamma(x)$. Unfortunately the rate is very small, c.f. Tab. 3.

In Fig. 8 we show the $p_\perp$ distributions of various inelastic J/ψ production processes at HERA, i.e. for $ep \rightarrow J/\psi + X$ at $\sqrt{s} = 314\,\mathrm{GeV}$. The resolved photon contributions (30,32) have a softer $p_\perp$ spectrum than the direct process (11). The contribution of J/ψ's from b decays stays always below the direct contribution. This is in contrast to the finding in [9] where the influence of the Q^2 dependence on the $p_\perp$ distribution was neglected. The resolved photon processes are dominant in the low z region whereas the direct process dominates at large z (see Fig. 12). Cutting at $z \sim 0.2$ a rather clean direct photon sample can be obtained. A clean resolved photon sample can, however, only be obtained by further cuts, e.g. by tagging the hadronic remnant of the photon. We note that experimentally the separation via a z cut is more involved because the reconstructed z value may differ substantially from the generated one. We shall discuss this problem in more detail in the next section.

We end this section by summarizing the various total cross sections in Tab. 3. The cross

[9] calculated by J. Terron

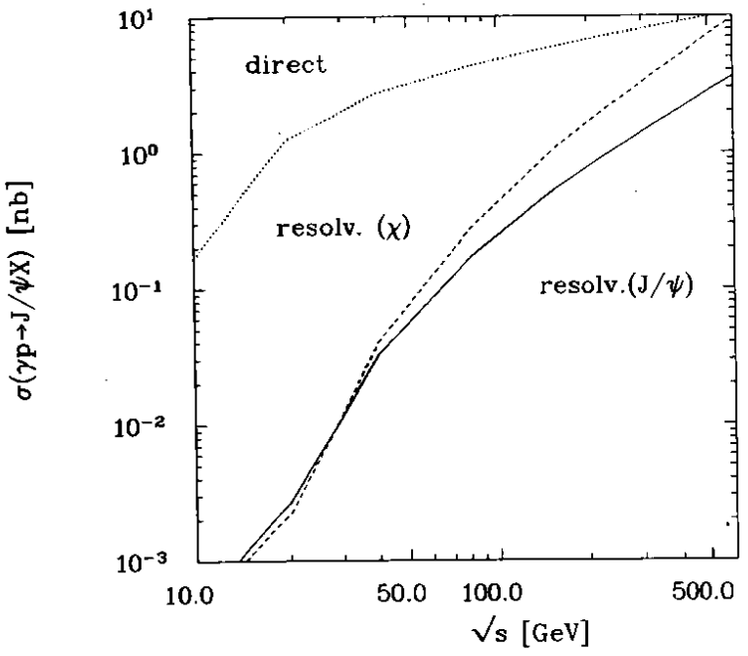

Figure 7: Cross sections of inelastic photoproduction of J/ψ's as a function of the CM energy. Dotted line: direct photon contribution as given in the CS model (11); solid line: resolved photon contribution (30); dashed line: resolved photon contribution (32).

Process	$\gamma g \to J/\psi g$		$\gamma g_{\mathbb{P}} \to J/\psi g$
	B1	B2	
$\sigma(p_\perp^{J/\psi} \geq 1$ GeV)	1.05 nb	1.32 nb	0.13 nb

$gg \to J/\psi g$	χ-decays	b-decays	$c\bar{c}J/\psi$	$gg \to J/\psi\gamma$	$\gamma\gamma \to \chi_2(\to J/\psi\gamma)$
0.09 nb	0.11 nb	0.07 nb	0.16 nb	0.023 nb	0.001 nb

Table 3: Contributions to the electroproduction of J/ψ at HERA. The cut $P_\perp^{J/\psi} \geq 1$ GeV has been applied but no K factor. The parametrization set B1 of Morfin and Tung is used if not stated otherwise.

section for double charm production (35) was calculated recently in [24].[10] This process could provide a clean signature when charmed hadrons are observed in addition to the J/ψ. The J/ψ production via two photon collisions is rather small.

[10] This process is implemented in EPJPSI 2.0 [27]

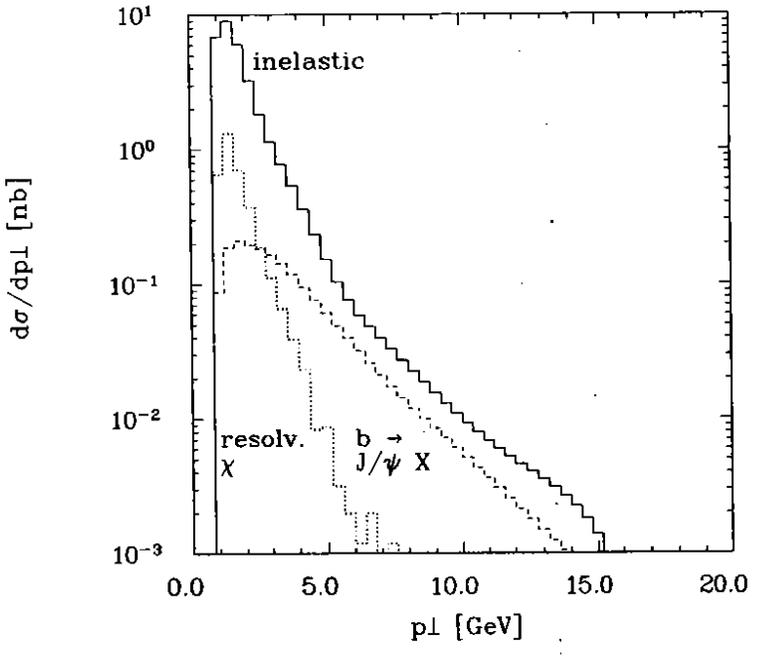

Figure 8: Transverse momentum distribution of various inelastic J/ψ production processes at HERA. Solid line: direct photon contribution in the CS model (11); dotted line: resolved photon contributions ($g\,g \to \chi\,g$); dashed line: J/ψ from b decays. The cut $p_\perp \geq 1$ GeV was applied.

3 Extraction of the Gluon Density

Here we shall describe how the gluon density in the proton can be measured in inelastic J/ψ production at HERA. From our investigations in section 2.4 we can estimate the cuts that define a safe region of truly inelastic J/ψ production. These cuts are $z < 0.9$, $p_\perp^{J/\psi} > 1$ GeV and $M^2 > 10\,\mathrm{GeV}^2$ and can also be applied to the respective reconstructed quantities despite of systematic shifts (see below). The relevant main contributing processes are then direct inelastic production, resolved photon contributions (30) and (32), J/ψ's from b decays and double charm production. Within the above cuts direct inelastic production is given by the CS model (11). As we shall see the further cut $z_{rec} > 0.2$ leaves us with a rather clean sample of direct J/ψ production. The gluon distribution can now be measured in two ways.

The gluon distribution can be constrained from an inclusive measurement of J/ψ production. Such an analysis was studied in [25] where it was observed that $d\sigma/dy$ is strongly correlated with the shape of the gluon distribution. Such a determination of a parton distribution function has to be iterative in general. It has, however, the advantage that it can also be applied in next-to-leading order (NLO) (provided the corresponding formula has been calculated). Of course, one has to rely on the fact that it is a background free data sample

to which one fits the ansatz for the parton distribution functions.

Here we try to reconstruct the gluon momentum fraction x_g explicitly and in turn to extract the gluon density. Such a procedure is limited to the leading order accuracy only but provides much more information about the production mechanism and also about the background processes. Such an explicit reconstruction of the gluon momentum has already been used by [4] but without including the resolved photon processes, which become important at HERA energies.

The general structure of the cross section at NLO is the following:

$$\frac{d^4\sigma(ep \to J/\psi + X)}{dy\, dQ^2\, dp_\perp^2\, dz} \sim \int ds_2\, G(x_g,\mu^2) \left\{\delta(s_2)\left[T^B + \frac{\alpha_s}{\pi} T^{V+S}\right] + \frac{\alpha_s}{\pi} T_g^F\right\} + \int ds_2\, q(x_g,\mu^2) \frac{\alpha_s}{\pi} T_q^F \tag{36}$$

At leading order there is the gluon initiated contribution, T^B, only. At NLO there are virtual and soft corrections to it (T^{V+S}) as well as real corrections, T_g^F. Also there are contributions from quark initial states, T_q^F. We denote by $\sqrt{s}$ the total CM energy, by $\sqrt{\hat{s}}$ the photon parton CM energy and by $\sqrt{s_2}$ the invariant mass of the partonic final state excluding the J/ψ. For the Born reaction (11) this remaining system is simply a gluon (g_2) and correspondingly $s_2 = 0$ ($s_2 = p_2^2$). The relation between $\hat{s}$, s_2 and x_g is:

$$\begin{aligned} \hat{s} &= \frac{p_\perp^2 + (1-z)m_{J/\psi}^2 + z\, s_2}{z(1-z)} \\ x_g &= \frac{\hat{s} + Q^2}{y\, s} \end{aligned} \tag{37}$$

Several comments are necessary:

- At NLO accuracy there are both gluon and quark initiated processes. The gluon and quark distribution functions have to be fitted simultaneously.
- The definition x_g depends on s_2. One can still reconstruct x_g, provided one splits the cross section into two pieces. For one contribution s_2 is small enough ($s_2 < \delta$) so that the Born kinematics can be applied. For the other contribution, s_2 is large enough so that it can be reconstructed experimentally. Then x_g is given according to (37). Symbolically we can write:

$$\begin{aligned} \sigma^{NLO} &= \int_0^\delta ds_2\, A(s_2) + \int_\delta^{s_2^{max}} ds_2\, B(s_2) \\ &= k(\delta)\ \sigma^{LO} + \int_\delta^{s_2^{max}} ds_2\, B(s_2) \end{aligned}$$

  In principle, the K - factor can depend on y, Q^2, $p_\perp^2$, z and $\sqrt{s}$ besides δ. Lacking the full NLO calculation, we assume K to be constant. In the case of open heavy flavour production, this is known to be a good approximation [7,8].
- One has to be very careful in the definition of invariants and scaling variables.

As an example of the last comment consider photon gluon fusion into J/ψ plus gluon where the incoming gluon has radiated another gluon before participating in the hard reaction (so called initial parton shower), i.e.

$$g_1 \to g_2 + g_3 \quad , \quad g_2 + \gamma \to J/\psi + g_4 \tag{38}$$

Then gluon g_2 will have a transverse momentum with respect to gluon g_1 and in turn with the proton. Thus the transverse momentum $p_\perp$ of the J/ψ in the CMS of g_2 and the photon will differ from its laboratory $p_\perp$. This was observed in [26] where the initial parton shower approach has been taken into account. But also the definition of $z = (p \cdot p_{J/\psi})/(p \cdot q)$ will be different depending on whether p is the momentum of g_2 or the momentum of g_1 (or of the proton). One also has to realize that a parton shower approach will overestimate the $p_\perp$ of g_2 since a $p_\perp$ cut-off is needed. The NLO calculation, in contrast, receives large contribution at small s_2, i.e. at small $p_\perp$ of gluon g_2.

In the following we restrict ourselves to a determination of the gluon density in leading order. If the scattered electron is integrated out (no-tag events), then Q^2 is typically very small. Therfore we take

$$Q^2 \approx Q^2_{rec} = 0\,. \tag{39}$$

Furthermore we expect s_2 to be a steeply falling function. Then we can assume that $p_\perp$ of g_2 is small enough such that

$$p_\perp^{J/\psi}(\text{Lab}) \sim p_\perp^{J/\psi}(\gamma g\ \text{CMS})$$

is a reasonable approximation.[11] Then we reconstruct x_g from (37) with $s_2 = 0$. To this end we have to determine y, $p_\perp \equiv p_\perp^{J/\psi}$ and z. The partonic CM energy $\sqrt{\hat{s}}$ can well be measured in $J/\psi \to l\bar{l}$ events through measurements of $p_\perp(l\bar{l}) = p_\perp(J/\psi)$ and $z(l\bar{l}) = z(J/\psi)$.

We note that the method of [25] is equivalent of approximating $\hat{s}$ by its average value and only determining y. Since the $c\bar{c}$ is in a bound state the $\hat{s}$ distribution is limited and peaked at an average value of $\bar{\hat{s}} = 22\ GeV^2$ (Fig. 9). This is exactly the value quoted in [25]:

$$\bar{x}_g = 2.3\, m_{J/\psi}^2/(y\, s) = 22\,\text{GeV}^2/(y\, s)$$

For the analysis we generate complete event samples[12] for inelastic J/ψ production via (11), (30), (31), (32), (34) and (35) with full hadronization using the LUND string fragmentation. All events were passed through a detector simulation program either of the H1 or ZEUS type. The J/ψ's are identified using the decay leptons reconstructed in the tracking system. All oppositely charged track pairs with $p_l \geq 0.5\ GeV$ are considered within an invariant mass range of $2.7\ GeV \leq m_{ll} \leq 3.5\ GeV$ where the most probable J/ψ candidate is the one which minimizes $|m_{ll} - m_{J/\psi}|$. From the momenta of the lepton pair the momentum of the J/ψ is calculated. In order to rely on the perturbative calculation of the CS model we require (the reconstructed) $p_\perp \geq 1\ GeV$.

The energy fraction of the photon

$$y = \frac{p \cdot q}{p \cdot l} \underbrace{=}_{\text{Lab}} \frac{(E + p_L)_\gamma}{(E + p_L)_e} \tag{40}$$

[11] We neglect $B(s_2)$.

[12] Two independent Monte Carlo generators, EPJPSI 2.0 [27] and a generator written by J. Terron have been used.

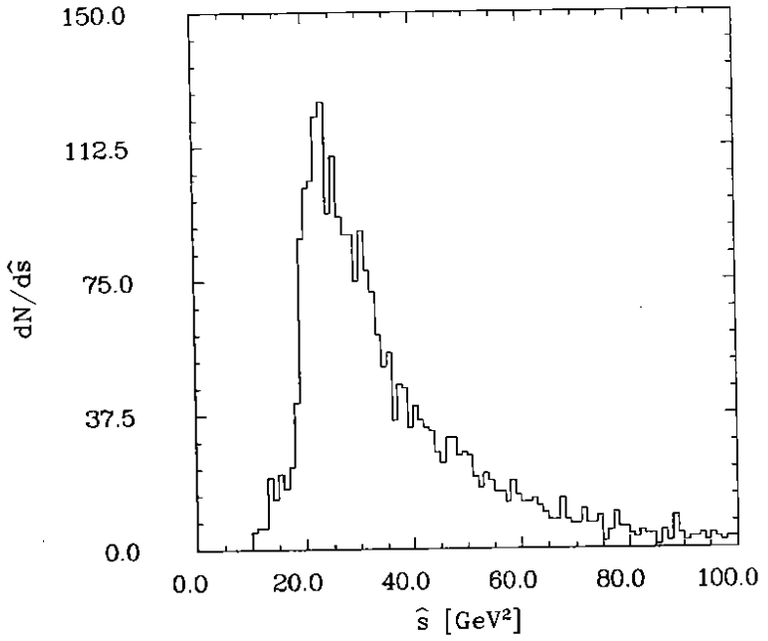

Figure 9: Invariant mass distribution for inelastic J/ψ production via $\gamma g \to J/\psi g$ at HERA energies ($z \leq 0.9$ and $p_\perp \geq 1$ GeV).

is reconstructed using the Jacquet Blondel method:

$$y_{rec} = \sum_h \frac{(E + p_L)_h}{2E_e} \tag{41}$$

where the sum runs over all particles measured in the calorimeter except the scattered electron. We show in Figs. 10 and 11 the correlation y vs. y_{rec} for J/ψ production via the direct process (10) and the resolved photon processes (30, 31, 32).

The scaled J/ψ energy

$$z = \frac{p \cdot p_{J/\psi}}{p \cdot q} \underbrace{=}_{\text{Lab}} \frac{(E + p_L)_\Psi}{(E + p_L)_\gamma} . \tag{42}$$

can be reconstructed from the momentum $p_{J/\psi} = p(l\bar{l})$ of the J/ψ and the variable y using

$$z_{rec} = \frac{p \cdot p_{J/\psi}}{y\,(p \cdot l)} = \frac{(E + p_L)_{J/\psi}}{2\,y_{rec}\,E_e} . \tag{43}$$

The reconstructed z distributions can be found in Fig. 12, where they are plotted together with the Monte Carlo results. From Fig. 10 we find that y can very well be reconstructed over the whole y range using (41) for the direct production channel. For this process also the reconstructed z distribution approximates the true (Monte Carlo) distribution very well over

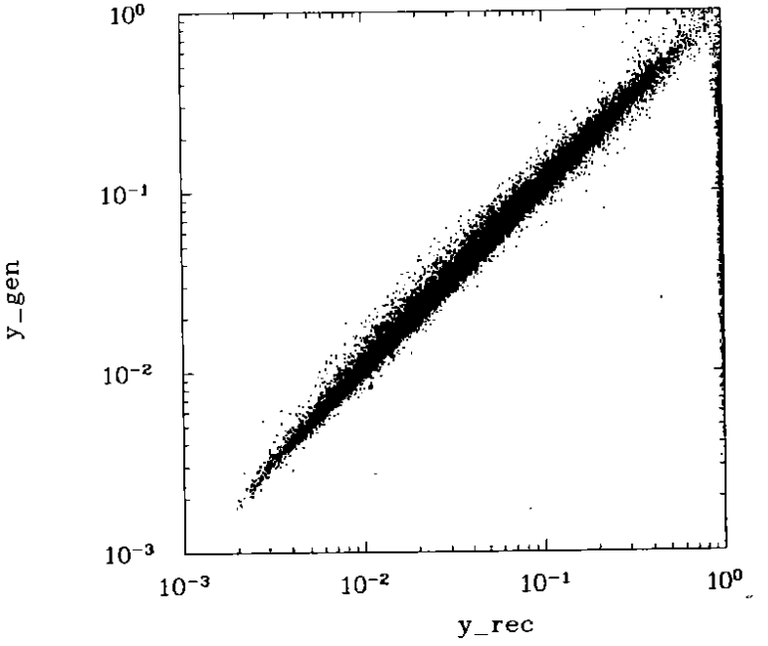

Figure 10: The correlation y vs. the reconstructed y_{rec} for inelastic J/ψ production at HERA via the direct process (11).

the whole z range except near $z = 0$. For J/ψ's produced via the hadronic component of the photon the reconstruction method does not work too good, the reason being the spectator jet of the photon. In fact, we have to distinguish the following cases for the resolved photon contributions:

- The photon remnants are fully contained in the calorimeter. Then the measurement (41) reconstructs y (40), the energy fraction carried by the photon. Also (43) approximates z as defined in (42). Thus the reconstructed z distribution follows the exact one. This is the region z close to zero in Fig. 12.

- The photon remnants are completely lost into the beam pipe. Then (41) gives the energy fraction carried by that parton p^γ within the photon which participated in the hard interaction, $y_{rec} \approx y_p$ with

$$y_p = \frac{(E + p_L)_{p^\gamma}}{2\,E_e} = x_p\,y\,. \tag{44}$$

Here x_p denotes the momentum fraction of the photon carried by the parton. Since $0 < x_p < 1$ we have $y_{rec} \approx y_p < y$. Consequently a parton-z_p is reconstructed

$$z_p = \frac{p \cdot p_{J/\psi}}{p \cdot p_{p^\gamma}} \underbrace{=}_{\text{Lab}} \frac{(E + p_L)_\Psi}{(E + p_L)_{p^\gamma}} = \frac{z}{x_p} > z\,. \tag{45}$$

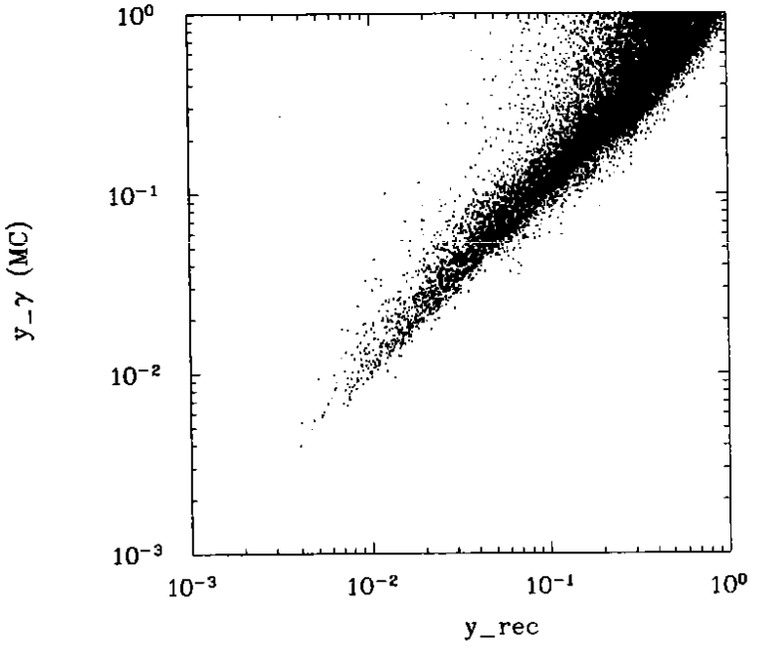

Figure 11: The correlation y vs. the reconstructed y_{rec} for inelastic J/ψ production at HERA via the hadronic component of the photon (30,31,32).

This is the region of $z > 0.75$ in Fig. 12. In this case the seen (reconstructed) subprocess is actually the one initiated by a parton inside the *photon* plus a parton inside the proton. If the latter parton is the gluon, then these events are really signal events as (10).

- The photon remnants are only partly reconstructed. Then (41) yields a value y_{rec} with $y_p < y_{rec} < y$. Correspondingly (43) yields a value z_{rec} with $z < z_{rec} < z_p = z/x_p$. This fills the region $0.2 \lesssim z \lesssim 0.75$ in Fig. 12.

Which of the above mentioned situations occurs depends on the acceptance of the calorimeter and the details of the fragmentation of the photon structure function which are far from being understood. In Fig. 13 we compare for the resolved photon contributions y_{rec} versus y_p for events where the photon remnant is not seen in the detector. It seems that at least in our simulation there is a good correlation between the reconstructed and the partonic y's. Note also that the photon remnants are usually flying backwards (i.e. keeping the direction of the incoming electron) in contrast to the proton remnants which follow the incoming proton direction.

In order to discriminate against double charm, resolved photon, diffractive and elastic J/ψ production we apply a cut on the reconstructed z besides the cut $p_\perp > 1\,\mathrm{GeV}$:

$$0.2 \leq z_{rec} \leq 0.9$$

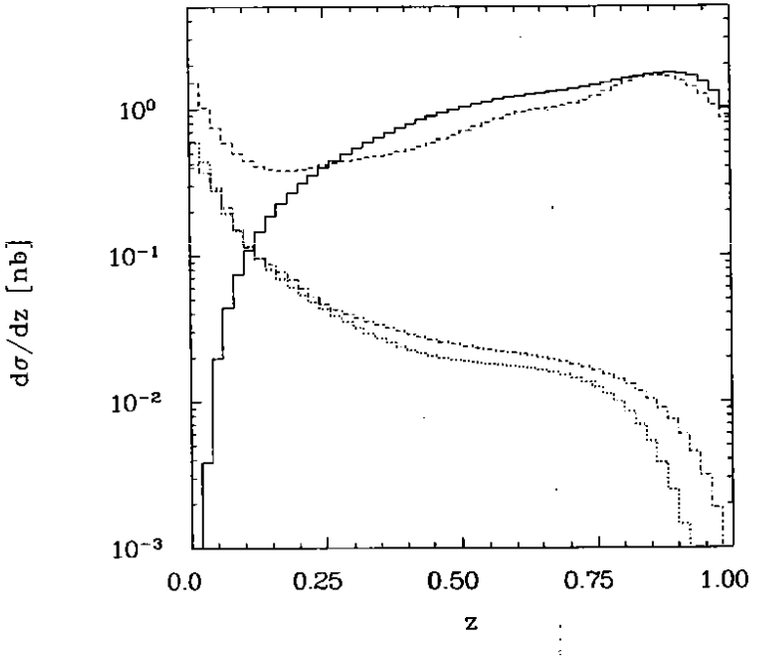

Figure 12: Distributions in the variable z for J/ψ events after demanding that they can be reconstructed in the tracking system and after a cut $p_\perp^{J/\psi} > 1\,\mathrm{GeV}$. Monte Carlo results for the direct process (11) as solid line, for the hadronic component of the photon (30,31,32) in dots. Distributions in the reconstructed z_{rec} in dashes for the direct channel and in dash-dots for the resolved photon one.

Cut	Signal direct γ	background resolved γ
$\lvert\cos\theta_{l\bar{l}}\rvert \leq 0.98; p_\perp^{J/\psi} \geq 1\,\mathrm{GeV}$	130 pb	8 pb
$0.2 < z < 0.9$	86 pb	3 pb

Table 4: Signal (11) and background rates after cuts, including $BR(J/\psi \to l^+l^-) = 0.14$, using the gluon density B1 of Morfin-Tung and without K-factors.

In principle one could further discriminate at least against the background from χ production by tagging on the photon in the decay, on the lines of [28]. However, present knowledge of the fragmentation of the spectator jet from the photon is inadequate .

In Tab.4 the accepted rates for the different selection criteria are shown for signal and background processes separately. After all the cuts the signal to background ratio S/B = 29.

Having reconstructed y and $\hat{s}$ we can determine x_g from eq.(37). The quality of this

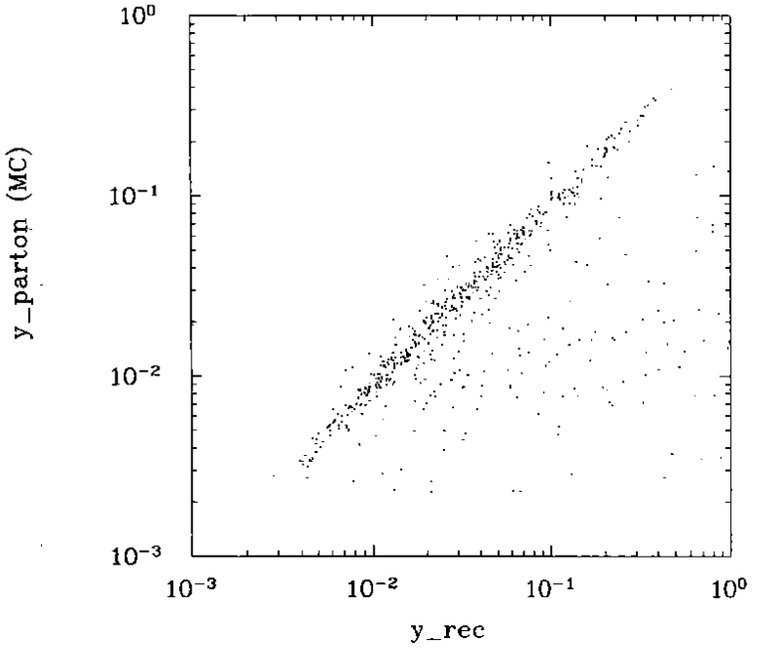

Figure 13: The correlation y_p eq.(44) vs. the reconstructed y_{rec} for J/ψ production via the hadronic component of the photon for events where the photon remnant is not seen in the detector.

reconstruction is shown in Fig. 14 and Fig. 15 where we plot x_g vs. $x_{g\,rec}$ and the distribution in the resolution $(x_g - x_g^{rec})/x_g$. We estimate that x_g can be determined with good quality ($\sigma = 0.06$) over the whole range

$$3 \times 10^{-4} < x_g < 1 \times 10^{-1} \qquad \text{at} \qquad < \mu^2 >= \hat{s} \tag{46}$$

The gluon density now can be determined from the measured distribution $d\sigma/dx_g$ by

$$G(x_g, \mu^2(x_g)) = \frac{d\sigma(x_g)/dx_g|_{exp}}{f(x_g)|_{MC}} \tag{47}$$

where $f(x_g)|_{MC} = 1/G(x_g)|_{MC}\, d\sigma/dx_g|_{MC}$ is determined by the Monte Carlo program. The reconstructed gluon density is shown in Fig. 16 and Fig. 17. The statistical errors for an integrated luminosity of $100\,pb^{-1}$ are shown by the vertical error bars in Fig. 16 and for $20\,pb^{-1}$ in Fig. 17. We also show the gluon density as obtained from different sets of the input gluon density and it can be seen that our method can clearly discriminate between these different parametrizations and provides a promising way of measuring the gluon density in ep collisions at HERA.

We conclude that with a integrated luminosity of 20 pb^{-1} HERA can provide a detailed measurement of the gluon density in inelastic J/ψ production. In Fig. 17 in addition recent

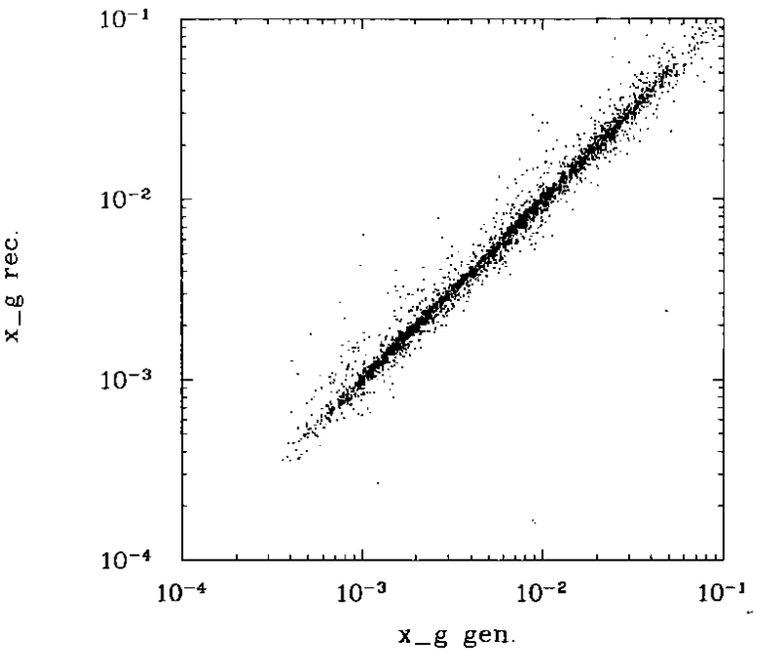

Figure 14: The correlation x_g vs. the reconstructed x_g^{rec} for J/ψ production via the direct process.

data from NMC are plotted to show the extension and the overlap of x_g measurements at very different energies.

4 Summary

In this work we attempted for the first time a complete description of photoproduction and leptoproduction of J/ψ mesons. This included various inelastic processes as well as elastic and diffractive reactions. All production mechanisms have been modeled. In addition, different models have been investigated for the dominant production mechanisms. The latter were found to be the following: (i) elastic J/ψ production leading to the exclusive J/ψ plus proton final state; (ii) diffractive dissociation of the proton (DD) where the photon couples to an off-shell J/ψ meson which is put on-shell by diffractive scattering of the proton which breaks up; and (iii) inelastic J/ψ production through photon gluon fusion where the photon couples directly to the gluon within the proton. Present day data from fixed target photo- and muonproduction experiments ($\sqrt{s} \leq 15\,\text{GeV}$) are well described by these three production mechanisms. We investigated total rates as well as distributions in transverse momentum $p_\perp$ (momentum transfer t) and scaled energy z of the J/ψ meson.

Starting from the successful description of existing low energy data we used our models to

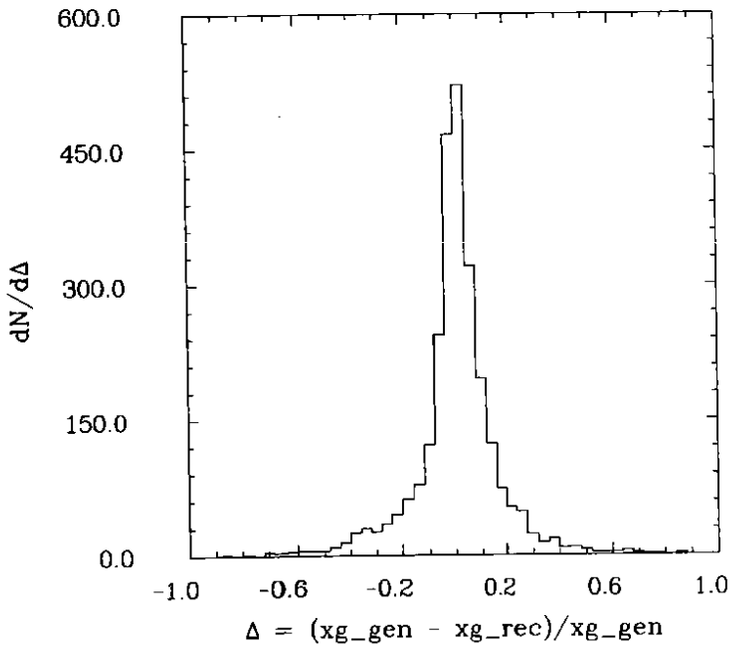

Figure 15: The resolution of the reconstructed x_g^{rec} for the direct process.

predict J/ψ production at higher energies. The possibility of measuring photoproduction of J/ψ mesons over a wide range of the photon energy ($\nu = \frac{ys}{2m_p}$) at HERA will allow detailed investigations of the various J/ψ production mechanisms. We found that the mechanisms that describe low energy data are the dominant ones at higher energies. From measurements of the elastic and DD reactions we expect useful information about the photon J/ψ coupling as well as about the nature of the Pomeron. We found that different pictures of its composition yield observable differences at HERA.

At this point we have to mention another possibility of determination of the partonic structure of the Pomeron. We predict diffractive inelastic J/ψ production to become sizeable at maximal HERA energies. Here the photon is diffractively dissociated into a J/ψ meson and a remaining hadronic system while the proton scatters quasi-elastically. Though this process is still small compared to inelastic J/ψ production via photon gluon fusion it should be measurable at HERA through it's unique signatures. These are a leading proton and/or the rapidity gap between the proton and the remaining hadronic system. Diffractive inelastic J/ψ production is a direct probe of the gluon content of the Pomeron.

At higher photon proton CM energies further (inelastic) production mechanisms become sizeable. Among them, "exotic" (i.e. interesting but small rate) processes like two photon production of J/ψ and the production of J/ψ in association with a hard photon. Additional sources of inelastic J/ψ production are b decays, double charm production, and resolved photon contributions. The latter offer the opportunity to measure the partonic content of

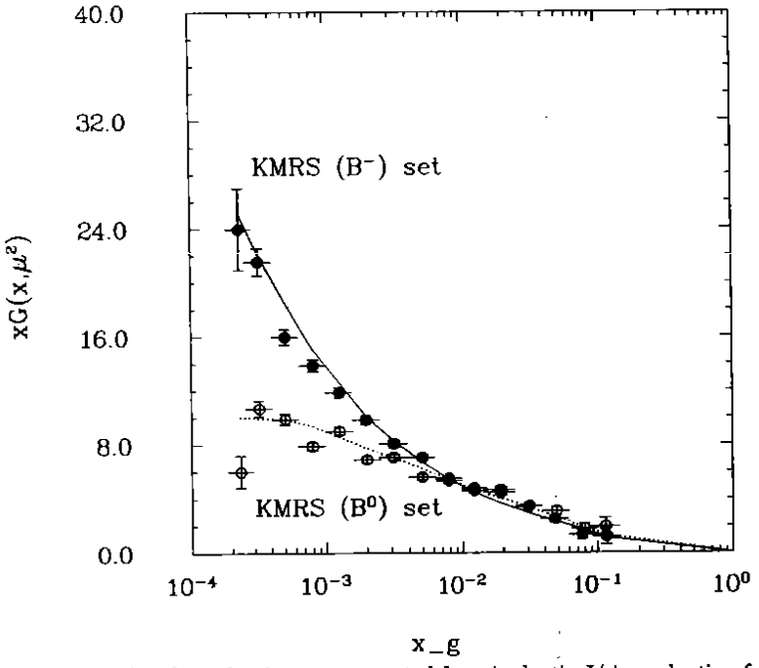

Figure 16: The gluon density reconstructed from inelastic J/ψ production for the input function of KMRS. The statistical error bars correspond to an integrated luminosity of $100\,pb^{-1}$ The curves show the input gluon density.

the photon. The main processes are $gg \to J/\psi g$ and $gg \to \chi g$ where the χ's then decay radiatively into a J/ψ. These resolved processes are thus a challenge to determine the gluon content of the photon which is thus far only poorly constraint. In this work we rather concentrated on the extraction of the gluon density within the proton.

To this end we studied in detail inelastic J/ψ production and it's transition region to diffractive production. Within the inelastic domain (defined through suitable cuts) contributions from elastic and diffractive J/ψ production mechanisms are small. We conclude that inelastic J/ψ production is well described through photon gluon fusion into a $c\bar{c}$ pair plus a gluon where the colour and spin constraints of the J/ψ are imposed on the $c\bar{c}$ system (the resolved photon contributions are, of course, to be added). Two approaches exist to transform the open charm state into the bound state J/ψ-meson. In the colour-singlet model the charmed quarks are treated non-relativistically as an s-wave system. The J/ψ wave function at the origin fixes the normalization. In the second approach the charmed quark pair is supposed to transform into a J/ψ if its mass is below the threshold of D-meson pair production. In both approaches inelastic J/ψ-production can be used to determine the proton gluon density: it enters the cross section already at the leading order. We found that either way correctly describes the low energy data in the inelastic domain. The theoretical systematic error in the gluon extraction can be estimated by comparing the results obtained with the

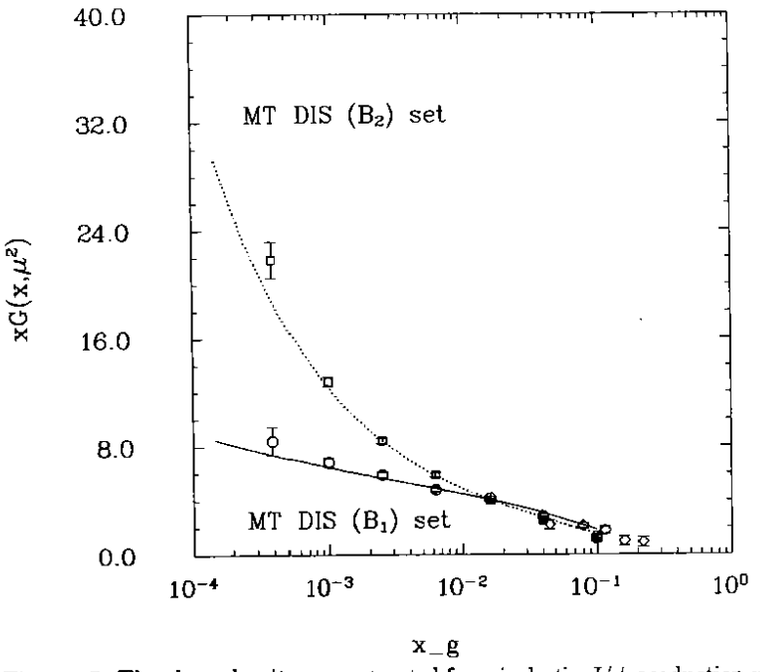

Figure 17: The gluon density reconstructed from inelastic J/ψ production using input functions of Morfin-Tung with statistical error bars corresponding to an integrated luminosity of $50\,pb^{-1}$ for set B1 and $20\,pb^{-1}$ for set B2. The curves show the input gluon density used. The points labeled as $\diamond$ show recent data of NMC.

two approaches. Eventually the complete next-to-leading order calculation to inelastic J/ψ production is needed. Effects of higher order QCD corrections on the reconstruction have been discussed in some detail in section 3.

We also want to note that we have assumed throughout the paper that the standard QCD evolution of structure function is valid down to the smallest x values ($\sim 10^{-4}$) that we encounter. More work is needed to investigate alternative scenarios describing the evolution at small x. A flattening out of the parton distribution functions at small x will show up in correspondingly smaller rates at small x. The effect of the partons being off-shell requires a new calculation of inelastic J/ψ production.

Finally we investigated how the gluon density of the proton can be extracted from inelastic J/ψ production at HERA. To this end we generated complete Monte Carlo events for all inelastic processes considered in this paper and passed them through detector simulation programs of both H1 and ZEUS type. We were able to obtain a clean sample of (Monte Carlo) events of J/ψ's produced through photon gluon fusion ($S/B \sim 29$). We estimate a range of $3 \times 10^{-4} \leq x_g \leq 0.1$ in which the gluon density of the proton can be measured at an average mass scale of the order of the J/ψ mass. We find an accuracy of about 10% at an integrated luminosity of $\sim 20^{-1}$ pb. This error contains the statistical error but does not

include any theoretical uncertainty. Given this small error we conclude that measurements of inelastic J/ψ events at HERA will allow for very detailed tests of the underlying dynamics and add further stringent constraints on the gluon content of the proton.

5 Acknowledgments

We want to thank all members of the Heavy Quark working group for the stimulating atmosphere of this workshop. We express our thanks to the members of the H1 and the Zeus collaboration. We are grateful to R. Eichler (ETH Zürich), D. Wyler (Univ. Zürich), S. Dangel (Univ. Zürich) and A. Salathe (Univ. Zürich) for drawing our attention to the gluon content of the pomeron. We also thank F. Barreiro for interesting discussions.

References

[1] B.H. Denby et al., FTPS collaboration, *Phys. Rev. Lett.* 52, 795 (1984).

[2] R. Barate et al., NA-14 Collaboration, *Z. Phys.* C33, 505 (1987).

[3] J.J. Aubert et al., EMC Collaboration, *Nucl. Phys.* B213, 1 (1983).

[4] M. de Jong, NMC Collaboration, *PhD Thesis* Utrecht (1991).
D. Allasia et al., NMC Collaboration, *Phys. Lett.* B258, 493 (1991).

[5] E.L. Berger and D. Jones, *Phys. Rev.* D23, 1521 (1981).

[6] R.Barbieri,R.Gatto,E.Remiddi, *Phys.Lett B* 106,497(1981)
W. Kwong, P.B. Mackenzie, R. Rosenfeld and J.L. Rosner *Phys. Rev.* D37, 3210 (1988).

[7] J. Smith and W.L. van Neerven, preprint ITP-SB-91-40;
R.K. Ellis and P. Nason, *Nucl. Phys.* B312, 551 (1989).

[8] P. Nason, S. Dawson and R.K. Ellis, *Nucl. Phys.* B303, 607 (1988); B327, 49 (1989); E. B335, 260 (1990);
W. Beenakker et al., *Phys. Rev.* D40, 54 (1989); *Nucl. Phys.* B351, 507 (1991).

[9] Z. Kunszt, *Phys. Lett.* B207, 103 (1988).

[10] H. Jung and D. Wyler, DESY preprint in preparation.

[11] G.A. Schuler and J. Terron, DESY preprint 92-017 (1992).

[12] H. Fritzsch and K.H. Streng, *Phys. Lett.* B72, 385 (1978);
D.W. Duke and J.F. Owens, *Phys. Lett.* B96, 184 (1980);
T. Tajima and T. Watanabe, *Phys. Rev.* D23, 1517 (1981).

[13] J.P. Leveille and T. Weiler, *Phys. Lett.* B86, 377 (1979).

[14] J.G. Morfin and Wu-Ki Tung, Fermilab-Pub-90/74 (1990).

[15] R.K. Ellis and Z. Kunszt, *Nucl. Phys* B303, 653 (1988).

[16] T. Sjöstrand, *Comp. Phys. Comm.* 39, 347 (1986);
T. Sjöstrand and M. Bengtsson, *Comp. Phys. Comm.* 43, 367 (1987).

[17] A. Donnachie and P.V. Landshoff, *Nucl. Phys.* B244, 322 (1984).

[18] G. Ingelman and P.E. Schlein, *Phys. Lett.* B152, 256 (1985).

[19] E.L. Berger, J.C. Collins, D.E. Soper and G.Sterman, *Nucl. Phys.* B286, 704 (1987).

[20] K.H. Streng, in Proc. of the workshop physics at HERA, Hamburg 1987, Ed. R.D. Peccei; also CERN preprint *CERN-TH* 4949, 1988.

[21] P.E. Schlein, talk presented at the Lepton Photon Symposium, Geneva 1991.

[22] M. Drees and K. Grassie, *Z. Phys.* C28, 451 (1985).

[23] M. Drees and C.S. Kim, DESY preprint 91-085 (1991).

[24] S.P. Baranov, in Proc. of the workshop on physics at HERA, Hamburg 1991, Eds. W. Buchmüller and G. Ingelman.

[25] S.M. Tkaczyk, W.J. Stirling and D.H. Saxon, in Proc. of the workshop on physics at HERA, Hamburg 1987, Ed. R.D. Peccei.

[26] R. Brugnera, in Proc. of the workshop on physics at HERA, Hamburg 1991, Eds. W. Buchmüller and G. Ingelman.

[27] H. Jung, in Proc. of the workshop on physics at HERA, Hamburg 1991, Eds. W. Buchmüller and G. Ingelman.

[28] B. van Eijk and R.Kinnunen, Z. Phys. C41 (1988) 489.